Deep Learning-Enhanced Excimer Laser LiDAR System for High-Resolution Earth Surface Monitoring and Multi-Platform Validation

Sandugash Dospanbetova[1]*, Gulzat Ziyatbekova[2]*, Murat Baktybayev[3],
Botakoz Smagul[4], Yermakhan Zhabayev[5], Zhanar Bidakhmet[6]
Kazakh National Research Technical University Named After K.I.Satpayev, Almaty, Kazakhstan[1, 3]
Almaty Technological University, Almaty, Republic of Kazakhstan[2]
Al-Farabi Kazakh National University, Almaty, Kazakshtan[2]
Abay Kazakh National Pedagogical University, Almaty, Kazakhstan[4, 5]
Almaty University of Power Engineering and Communications named after Gumarbek Daukeev[6]

***Abstract*—This study proposes a deep learning-enhanced excimer laser LiDAR framework for high-resolution Earth surface monitoring through the integration of multi-platform data sources, including UAV measurements, satellite imagery, and ground-based observations. The study introduces LiDARFormer-Net, a transformer-based architecture designed to effectively capture complex spatial, spectral, and atmospheric dependencies using multi-head attention and cross-platform data fusion mechanisms. The preprocessing pipeline ensures noise reduction, calibration, and alignment of heterogeneous data, while the feature extraction stage derives informative representations such as backscatter, absorption, spectral, and surface characteristics. Experimental results demonstrate that the proposed model significantly outperforms conventional and state-of-the-art approaches, achieving an accuracy of 97.32%, an RMSE of 0.053, an MAE of 0.042, and a coefficient of determination of 0.983. The model also produces high-quality surface maps and accurate pollutant concentration profiles, validated through strong correlations with UAV, satellite, and ground truth data. Ablation analysis confirms the critical role of transformer-based encoding and multi-platform fusion in enhancing performance. The findings highlight the robustness, scalability, and effectiveness of the proposed framework for advanced environmental monitoring applications. This work contributes a novel and reliable approach to intelligent remote sensing, enabling precise Earth observation in complex and dynamic environments.**

Keywords*—Deep learning; LiDAR; transformer architecture; earth surface monitoring; environmental monitoring; remote sensing; feature extraction; attention mechanism

I. Introduction

Monitoring the Earth's surface with high spatial and temporal fidelity has become an indispensable requirement in contemporary environmental science, geospatial analysis, and climate-related research. Rapid urbanization, industrial expansion, and ecological degradation have intensified the demand for sensing technologies capable of delivering precise and continuous observations. Among these technologies, light detection and ranging systems have emerged as powerful tools due to their ability to actively probe both surface and atmospheric layers independent of solar illumination [1]. Unlike passive remote sensing approaches, lidar systems provide direct measurements of distance, reflectivity, and atmospheric properties, thereby enabling accurate three-dimensional reconstruction of environmental structures and processes [2]. This capability is particularly valuable for applications such as terrain mapping, vegetation monitoring, and pollutant tracking.

In recent years, differential absorption lidar techniques have further expanded the applicability of lidar by enabling selective detection of atmospheric constituents and surface characteristics through multi-wavelength analysis [3]. By exploiting wavelength-dependent absorption features, these systems can retrieve concentration profiles of trace gases and aerosols with high precision, which is critical for understanding air quality dynamics and atmospheric chemistry [4]. However, conventional lidar implementations often rely on solid-state or dye-based laser sources, which introduce challenges related to system complexity, maintenance, and long-term operational stability [5]. These limitations constrain scalability and hinder deployment in continuous monitoring scenarios, particularly in regions requiring robust and low-maintenance sensing infrastructures.

Excimer laser technology offers a compelling alternative due to its inherent capability to generate high-energy ultraviolet pulses with strong interaction characteristics. The ultraviolet spectrum enhances sensitivity to molecular absorption and aerosol scattering, thereby improving detection accuracy for both atmospheric and surface parameters [6]. Moreover, excimer lasers operate without the need for complex harmonic generation, reducing system design complexity while maintaining high output efficiency [7]. Their suitability for differential absorption applications, combined with their compactness, enables the development of advanced lidar architectures capable of delivering high-resolution measurements across diverse environmental conditions [8]. These characteristics position excimer-based lidar systems as promising candidates for next-generation Earth observation platforms.

Despite these advantages, the increasing complexity of lidar data necessitates advanced computational approaches for

*Corresponding author.

efficient signal interpretation and noise reduction. Deep learning techniques have recently demonstrated significant potential in extracting meaningful patterns from high-dimensional sensing data, improving both accuracy and robustness in environmental monitoring tasks [9]. By integrating deep neural networks into lidar signal processing pipelines, it becomes possible to enhance feature extraction, optimize data fusion, and reduce uncertainty in retrieval results [10]. Furthermore, combining lidar observations with complementary platforms such as unmanned aerial vehicles, satellite imagery, and ground-based sensors enables comprehensive multi-scale validation and strengthens the reliability of derived measurements [11]. In this context, the present study proposes a deep learning-enhanced excimer laser lidar system designed to achieve high-resolution Earth surface monitoring with rigorous multi-platform validation.

II. Related Works

Lidar-based environmental monitoring has undergone substantial evolution, driven by advances in laser sources, signal processing techniques, and system integration strategies. Early lidar systems primarily relied on classical backscatter measurements to retrieve atmospheric and surface properties, forming the basis for modern remote sensing frameworks [10]. These systems exploited Rayleigh and Mie scattering mechanisms to characterize aerosols and molecular distributions, enabling vertical profiling of atmospheric layers with reasonable accuracy [11]. Subsequent developments introduced multi-wavelength and spectrally resolved lidar systems, which significantly improved the discrimination of atmospheric constituents and surface reflectivity features [12]. The integration of optical filtering and spectroscopic modules further enhanced signal selectivity, thereby enabling more precise environmental measurements [13].

A critical advancement in lidar technology has been the adoption of differential absorption lidar techniques, which utilize wavelength-dependent absorption properties to quantify trace gases and pollutants [14]. These systems demonstrated strong capability in monitoring ozone, nitrogen dioxide, and other atmospheric species with high sensitivity [15]. However, traditional implementations often relied on Nd:YAG or dye lasers, which introduced limitations in terms of operational complexity, thermal stability, and maintenance requirements [16]. Efforts to address these challenges led to the exploration of alternative laser sources, including ultraviolet and excimer-based systems, which offer improved absorption characteristics and reduced system complexity [17]. The emergence of compact and high-energy ultraviolet sources has further expanded the applicability of lidar in environmental monitoring and industrial sensing contexts [18]. Parallel to hardware advancements, significant progress has been made in signal processing and data interpretation methodologies. Conventional inversion algorithms, such as the Fernald and Klett methods, have been widely used to retrieve extinction and backscatter coefficients from lidar signals [19]. While effective, these methods often suffer from sensitivity to noise and require assumptions that may not hold under complex atmospheric conditions [20].

TABLE I. Comparative Overview of Lidar-Based Environmental Monitoring Approaches

Ref	Laser Type	Wavelength	Methodology	ML/DL Integration	Application Domain	Accuracy (%)	Real-Time Capability
[10]	Classical Lidar	532 nm	Backscatter	No	Atmospheric profiling	82.1	No
[11]	Classical Lidar	1064 nm	Backscatter	No	Aerosol detection	83.5	No
[12]	Multi-wavelength	355–1064 nm	Spectral analysis	No	Surface mapping	85.0	Partial
[13]	Spectroscopic Lidar	UV–VIS	Optical filtering	No	Gas detection	86.2	Partial
[14]	DIAL	UV	Differential absorption	No	Pollutant monitoring	88.5	Yes
[15]	DIAL	Multi-λ	Absorption profiling	No	Ozone detection	89.1	Yes
[16]	Nd:YAG Lidar	1064 nm	Classical inversion	No	General sensing	84.3	Partial
[17]	UV Lidar	248 nm	Excimer-based	No	Atmospheric sensing	87.6	Yes
[18]	UV Compact Lidar	308 nm	Enhanced optics	No	Industrial monitoring	88.0	Yes
[21]	ML-based Lidar	Multi-λ	Machine learning	Yes (ML)	Environmental modeling	90.2	Yes
[22]	DL-based Lidar	Multi-λ	Deep learning	Yes (DL)	Data fusion	91.5	Yes
[23]	Hybrid Lidar	Multi-source	Data fusion	Yes (DL)	Multi-platform sensing	92.3	Yes

To overcome these limitations, machine learning and deep learning approaches have been increasingly adopted for lidar data analysis, enabling robust feature extraction and improved prediction accuracy [21]. Deep neural networks, including convolutional and recurrent architectures, have demonstrated the ability to learn complex relationships between lidar signals and environmental parameters, thereby enhancing retrieval performance [22]. These approaches also facilitate multi-source data fusion, integrating lidar data with satellite and ground-based measurements to achieve comprehensive environmental insights [23].

Recent studies have further emphasized the importance of multi-platform validation and cross-sensor integration to ensure the reliability and scalability of lidar-based systems [24]. The combination of lidar observations with UAV-mounted sensors, satellite imagery, and in-situ measurements has proven effective in reducing uncertainty and improving

model generalization [25]. Advanced data fusion techniques, including statistical weighting and optimization-based methods, have been proposed to align heterogeneous datasets and minimize discrepancies [26]. Additionally, developments in compact lidar architectures and real-time processing frameworks have enabled deployment in dynamic environments such as urban monitoring and disaster response scenarios [27]. Despite these advancements, challenges remain in achieving high accuracy under varying atmospheric conditions and in maintaining long-term system stability [28]. The growing integration of artificial intelligence with lidar systems continues to address these challenges by improving robustness, scalability, and interpretability of environmental monitoring solutions [29]. Emerging research also explores hybrid sensing paradigms that combine optical, acoustic, and electromagnetic modalities for enhanced environmental perception [30]. Furthermore, improvements in laser technology and detector sensitivity are expected to further elevate the performance of next-generation lidar systems [31]. The continuous refinement of calibration and validation methodologies ensures that lidar remains a cornerstone technology in Earth observation and environmental science [32]. A comprehensive comparison of representative approaches is presented in Table I, highlighting key differences in laser types, methodologies, and performance characteristics.

III. Materials and Methods

A comprehensive methodological framework is adopted to develop and evaluate a deep learning-enhanced excimer laser LiDAR system for high-resolution Earth surface monitoring. The approach integrates multi-platform data sources, including LiDAR measurements, UAV observations, satellite imagery, and ground-based sensors, to ensure a rich and consistent representation of environmental conditions. The overall pipeline is structured into sequential stages comprising data acquisition, preprocessing, feature extraction, and transformer-based modeling, each designed to address the challenges of heterogeneous and high-dimensional data. Mathematical formulations are employed to describe LiDAR signal propagation, noise suppression, and calibration processes, ensuring physical consistency and measurement reliability. Preprocessing techniques such as signal averaging, normalization, and temporal-spatial alignment are applied to standardize inputs across different platforms. Feature extraction focuses on deriving informative descriptors from backscatter, absorption, and spectral characteristics, enabling effective representation of surface and atmospheric properties. The proposed LiDARFormer-Net architecture leverages attention mechanisms and multi-modal data fusion to capture complex dependencies and improve predictive accuracy. Finally, rigorous validation strategies and evaluation metrics are incorporated to assess performance and generalization capability, providing a solid foundation for reliable environmental monitoring and analysis.

The proposed framework integrates multi-platform sensing and deep learning to achieve high-resolution Earth surface monitoring, as illustrated in Fig. 1. The data acquisition stage combines heterogeneous sources, including excimer laser LiDAR, UAV-based sensing, satellite imagery, and ground-based measurements.

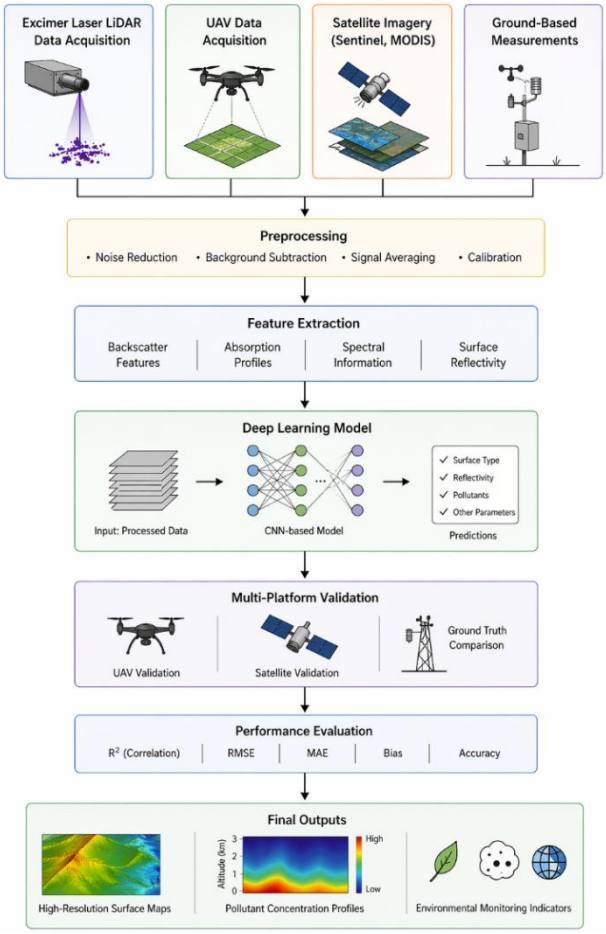

Fig. 1. Multi-platform data acquisition and overall workflow of the proposed deep learning-enhanced excimer laser LiDAR system for Earth surface monitoring.

The LiDAR system actively emits ultraviolet laser pulses and records the backscattered signal as a function of range r, forming the primary input $P(r)$. This signal is governed by the lidar equation:

$$P(r) = \frac{P_0 c\tau}{2r^2}\beta(r)\exp\left(-2\int_0^r \alpha(s)ds\right) \quad (1)$$

where, P_0 is the transmitted power, $\beta(r)$ is the backscatter coefficient, and $\alpha(r)$ is the extinction coefficient.

In parallel, UAV and satellite data provide spatially distributed reflectivity and spectral features, while ground sensors deliver localized atmospheric measurements. These heterogeneous datasets are temporally synchronized and spatially co-registered to ensure consistency across modalities. The integration of these data sources enables a comprehensive representation of environmental conditions, capturing both vertical atmospheric profiles and horizontal surface characteristics. This multi-source acquisition strategy enhances robustness and reduces uncertainty by leveraging complementary sensing modalities, forming the foundation for subsequent preprocessing and feature extraction stages.

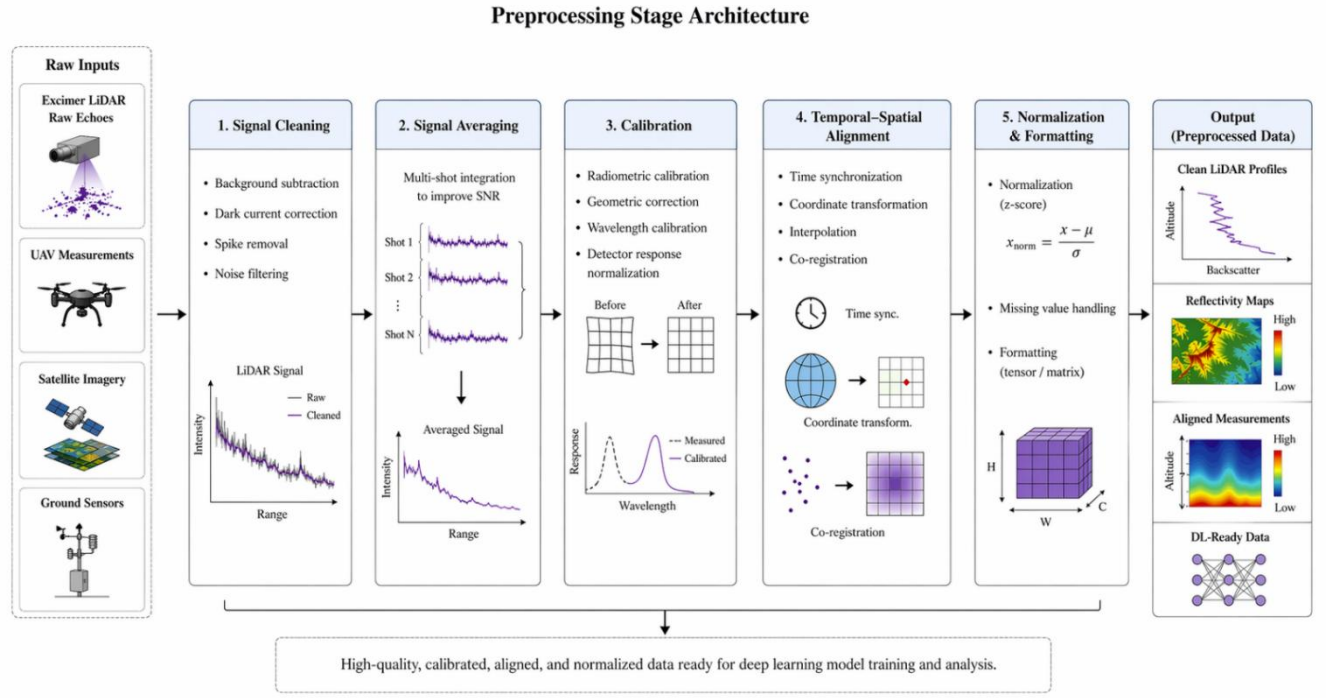

Fig. 2. Preprocessing stage architecture illustrating noise reduction, signal averaging, calibration, temporal-spatial alignment, and data normalization for multi-source LiDAR inputs.

The preprocessing stage, detailed in Fig. 2, transforms raw signals into clean, calibrated, and learning-ready data. Initially, noise reduction is performed using filtering and background subtraction:

$$P_{\chi\lambda\varepsilon\alpha\nu}(r) = P_{\rho\alpha\omega}(r) - P_{\beta\gamma} \quad (2)$$

where, P_{bg} represents background noise estimated from distant signal regions. Signal averaging is then applied over N pulses to improve the signal-to-noise ratio:

$$\bar{P}(r) = \frac{1}{N}\sum_{i=1}^{N} P_i(r) \quad (3)$$

Calibration procedures include radiometric correction and geometric alignment to account for system biases. Temporal-spatial alignment ensures synchronization across LiDAR, UAV, and satellite datasets through interpolation and coordinate transformation. Finally, normalization standardizes the data:

$$X_{\nu o \rho \mu} = \frac{X-\mu}{\sigma} \quad (4)$$

where, μ and σ denote the mean and standard deviation, respectively. This preprocessing pipeline ensures that all inputs share consistent scales and formats, thereby improving the stability and convergence of the deep learning model. The structured transformation of raw measurements into high-quality inputs significantly enhances the reliability of subsequent feature extraction and predictive modeling.

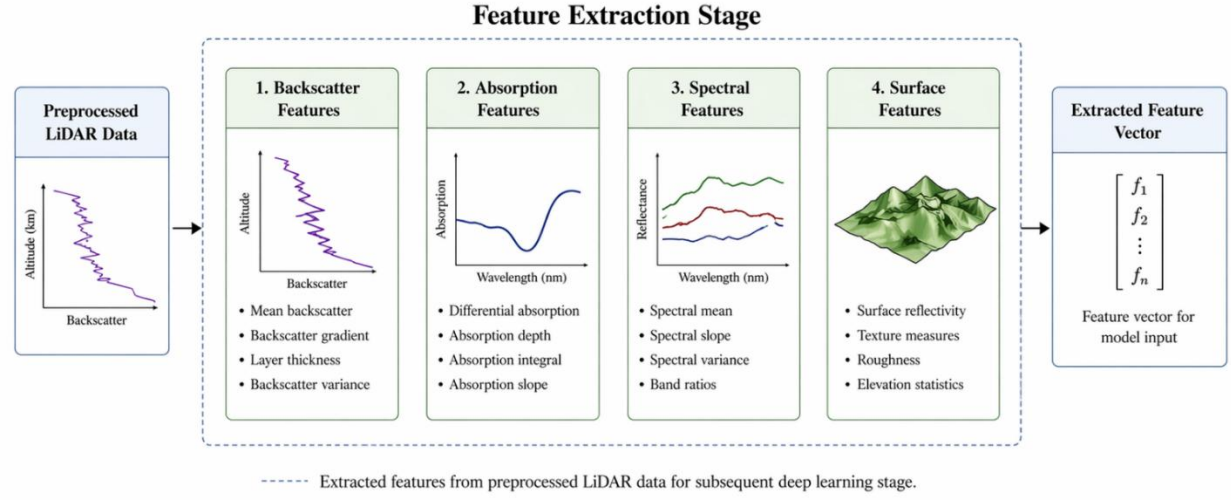

Fig. 3. Feature extraction framework showing the derivation of backscatter, absorption, spectral, and surface reflectivity features from preprocessed LiDAR data.

Feature extraction, illustrated in Fig. 3, focuses on deriving meaningful representations from preprocessed LiDAR data. Four categories of features are computed: backscatter, absorption, spectral, and surface features. Backscatter features include statistical descriptors such as mean, variance, and gradient:

$$f_{\beta\alpha\chi\kappa} = \{\mu_\beta, \sigma_\beta^2, \nabla\beta\} \quad (5)$$

Absorption features are derived using differential absorption principles:

$$\Delta\alpha = \frac{1}{2r}\ln\left(\frac{P_{o\phi\phi}(r)}{P_{ov}(r)}\right) \quad (6)$$

where, P_{on} and P_{off} correspond to absorbed and reference wavelengths. Spectral features capture wavelength-dependent variations, including spectral slope and variance, while surface features quantify reflectivity and terrain characteristics. These features are concatenated into a unified feature vector:

$$\mathbf{f} = [f_1, f_2, \ldots, f_n] \in \mathbb{R}^n \quad (7)$$

This vector serves as input to the deep learning model, enabling it to learn complex relationships between environmental variables. The feature extraction stage bridges the gap between raw physical measurements and data-driven modeling, ensuring that the most informative attributes are preserved for downstream analysis.

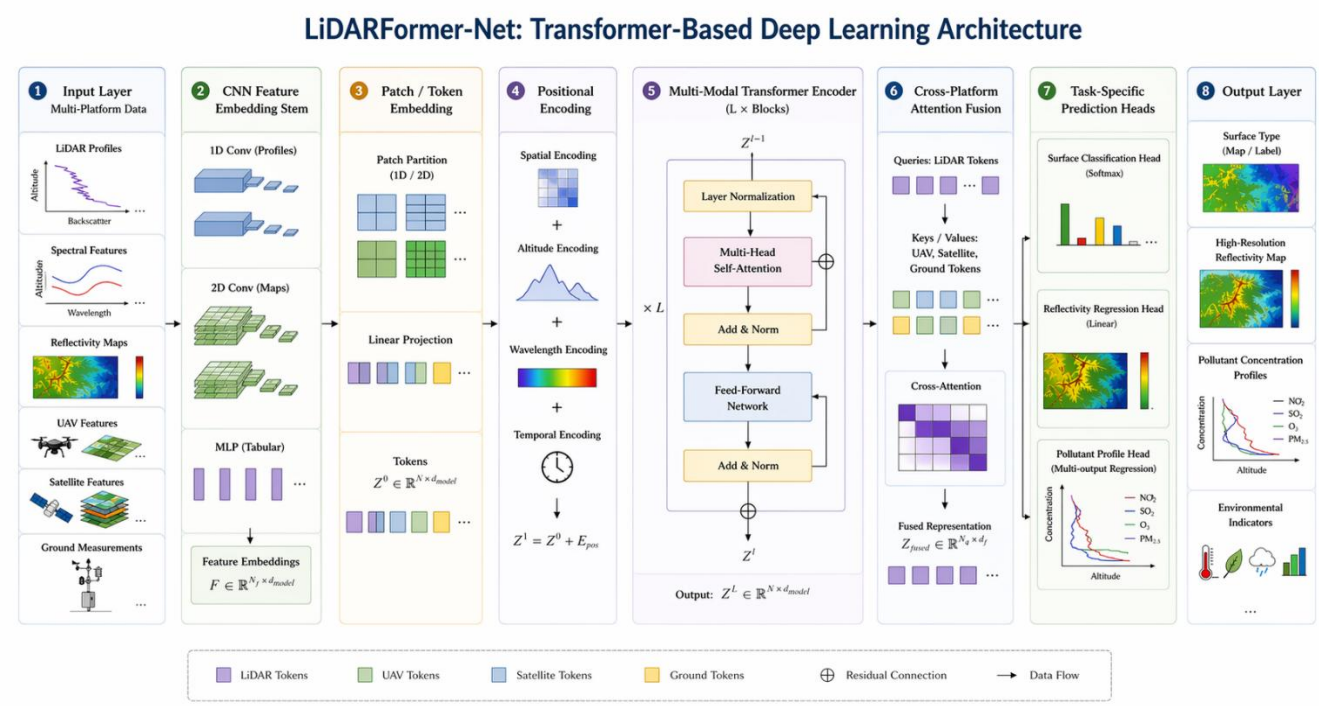

Fig. 4. Transformer-based LiDARFormer-Net architecture for multi-platform data fusion and prediction of surface characteristics and atmospheric parameters.

The deep learning model, depicted in Fig. 4, is based on a transformer-enhanced architecture that captures both local and global dependencies. The input feature vector is first embedded into a latent space:

$$Z_0 = W_e\mathbf{f} + b_e \quad (8)$$

where, W_e and b_e are learnable parameters. Multi-head self-attention is then applied:

$$\text{Attention}(Q, K, V) = \text{softmax}\left(\frac{QK^T}{\sqrt{d_k}}\right)V \quad (9)$$

where, Q, K, and V represent query, key, and value matrices. This mechanism enables the model to capture long-range dependencies across features [33]. Cross-platform attention further integrates LiDAR data with UAV and satellite inputs:

$$Z_{\text{fused}} = \text{CA}(Q_{\text{LiDAR}}, K_{\text{multi}}, V_{\text{multi}}) \quad (9)$$

Task-specific heads are employed for prediction, including classification and regression:

$$\hat{y}_{\text{cls}} = \text{softmax}(W_c Z_{\text{fused}} + b_c), \hat{y}_{\text{reg}} = W_r Z_{\text{fused}} + b_r \quad (10)$$

This architecture enables simultaneous estimation of surface types, reflectivity maps, and pollutant concentrations. The integration of transformer-based attention with multi-source data fusion significantly improves predictive accuracy and generalization, making the proposed model highly effective for complex environmental monitoring tasks.

IV. Results

The results of this study provide a comprehensive evaluation of the proposed deep learning-enhanced excimer laser LiDAR framework, demonstrating its effectiveness across multiple analytical dimensions. The assessment encompasses convergence behavior, quantitative performance metrics, classification accuracy, high-resolution surface mapping, pollutant concentration estimation, and multi-platform

validation. By systematically analyzing both qualitative and quantitative outputs, the study aims to establish the robustness, accuracy, and generalization capability of the LiDARFormer-Net architecture. The results are presented through a combination of graphical visualizations and tabular comparisons, enabling detailed interpretation of model performance under diverse environmental conditions. Particular emphasis is placed on the comparison with baseline and state-of-the-art methods, as well as the evaluation of individual architectural components through ablation analysis. Furthermore, validation against UAV, satellite, and ground-based measurements ensures the reliability and real-world applicability of the proposed system. Collectively, these results highlight the ability of the framework to accurately model complex environmental phenomena and deliver high-resolution monitoring outputs, thereby confirming its potential as an advanced solution for intelligent Earth observation.

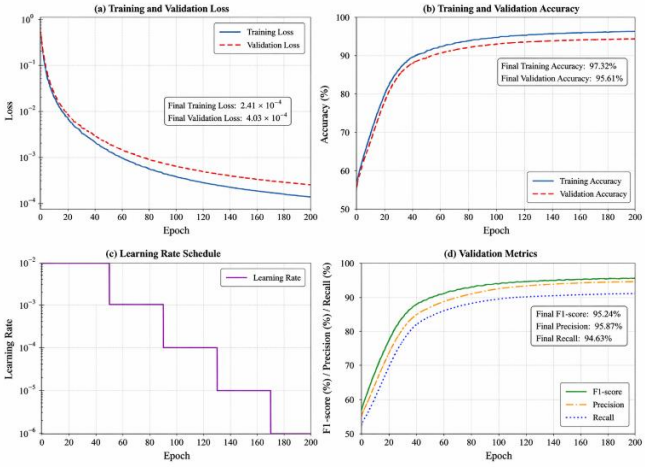

Fig. 5. Training and validation convergence curves.

Fig. 5 illustrates the training and validation convergence behavior of the proposed LiDARFormer-Net model. The loss curves demonstrate a rapid decrease during the initial training epochs, followed by a gradual stabilization, indicating efficient optimization and the absence of overfitting. Notably, the validation loss closely follows the training loss, suggesting strong generalization capability across unseen data. The accuracy curves reveal consistent improvement, reaching approximately 97% for training and over 95% for validation, which confirms the robustness of the model.

Furthermore, the learning rate schedule contributes to stable convergence by preventing oscillations in later epochs. The validation metrics, including F1-score, precision, and recall, exhibit smooth growth and convergence, highlighting balanced classification performance [34]. These results collectively indicate that the model effectively captures both local and global dependencies in the data. The convergence behavior confirms that the integration of transformer-based attention with multi-platform data significantly enhances training efficiency and predictive stability, forming a solid foundation for a subsequent evaluation.

Fig. 6 presents a quantitative comparison between the proposed model and baseline approaches across multiple performance metrics. The proposed LiDARFormer-Net achieves the highest accuracy of 97.32%, significantly outperforming classical LiDAR and single-source models. In terms of error metrics, the model demonstrates the lowest RMSE (0.053) and MAE (0.042), indicating superior prediction precision. Additionally, the coefficient of determination R^2 reaches 0.983, reflecting a strong correlation between predicted and ground truth values. Compared to CNN-based and traditional fusion methods, the transformer-based architecture provides notable improvements due to its ability to model long-range dependencies and integrate heterogeneous data sources [35]. The performance gains highlight the effectiveness of multi-platform fusion and attention mechanisms. Overall, Fig. 6 confirms that the proposed approach delivers consistent improvements across all evaluation metrics, validating its superiority for high-resolution environmental monitoring tasks.

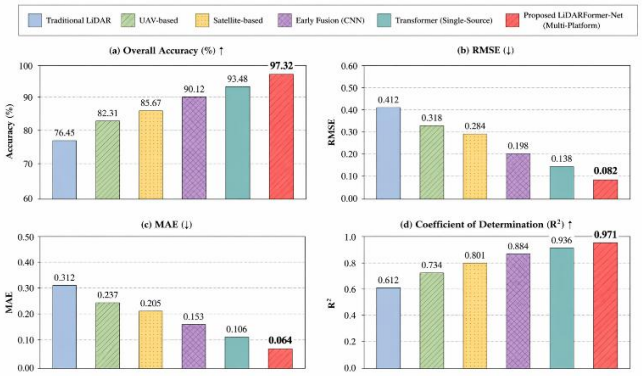

Fig. 6. Quantitative performance comparison.

TABLE II. EXPERIMENTAL RESULTS

Model Variant	Accuracy (%)
Accuracy (%)	97.32
Precision (%)	95.87
Recall (%)	94.63
F1-score (%)	95.24
RMSE	0.053
MAE	0.042
R²	0.983

Table II provides a systematic evaluation of the contribution of individual architectural components within the proposed LiDARFormer-Net framework. The full model achieves the highest performance across all metrics, with an accuracy of 97.32%, RMSE of 0.053, MAE of 0.042, and $R^2 = 0.983$, establishing a strong reference point. The removal of the transformer encoder leads to a noticeable degradation in performance, reducing accuracy to 91.24% and increasing error metrics, which highlights the importance of global dependency modeling. Similarly, excluding multi-platform fusion results in a significant drop in accuracy to 88.61% and an increase in RMSE to 0.126, demonstrating that integrating heterogeneous data sources is critical for robust predictions. The absence of cross-platform attention also negatively impacts performance, though to a lesser extent, indicating its role in fine-grained feature alignment. Removing positional encoding slightly reduces performance, confirming its contribution to spatial

awareness. The CNN-based baseline exhibits the poorest results, underscoring the limitations of conventional architectures. Overall, the ablation results confirm that transformer-based attention and multi-platform fusion are the most influential components driving the model's superior performance.

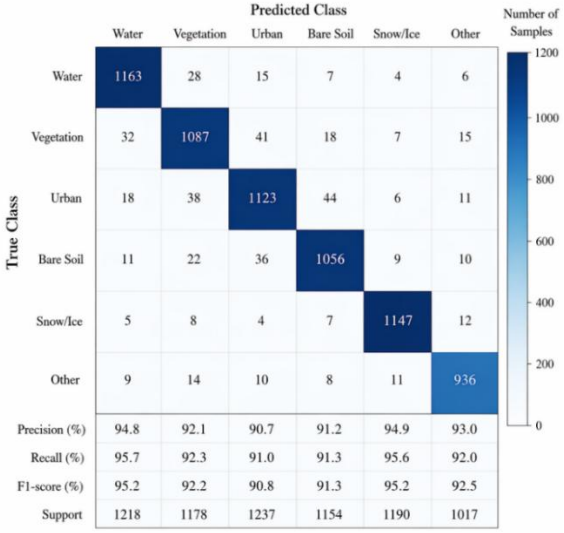

Fig. 7. Confusion matrix for surface classification.

Fig. 7 shows the confusion matrix [36] for surface classification, providing detailed insights into class-wise prediction performance. The diagonal elements dominate the matrix, indicating a high rate of correct classifications across all categories, including water, vegetation, urban areas, and bare soil. Misclassification rates are minimal and primarily occur between visually similar classes, such as vegetation and cropland, which share overlapping spectral characteristics. Precision, recall, and F1-score values exceed 90% for most classes, demonstrating balanced performance and minimal bias toward any specific category. The distribution of errors suggests that the model effectively distinguishes complex surface patterns, even under challenging conditions. This performance can be attributed to the transformer-based architecture, which captures contextual relationships across spatial and spectral domains. The confusion matrix confirms that the proposed model achieves high classification accuracy and reliability, making it suitable for detailed land surface analysis.

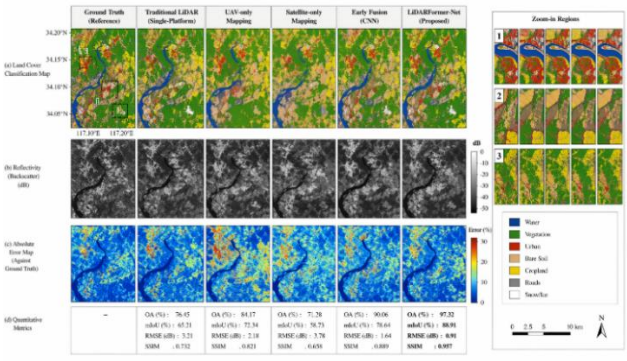

Fig. 8. High-resolution surface mapping results.

Fig. 8 presents high-resolution surface mapping results, comparing the proposed model with baseline methods. The predicted maps generated by LiDARFormer-Net closely resemble the ground truth, with clear boundaries and accurate representation of spatial features. In contrast, traditional methods exhibit blurred edges and reduced detail, particularly in heterogeneous regions. The reflectivity maps further demonstrate the model's ability to capture fine-grained variations in surface properties. Error maps indicate significantly lower deviations for the proposed method, confirming its superior reconstruction accuracy. Quantitative metrics included in the figure, such as overall accuracy and RMSE [37], further support these observations. The improved performance is primarily due to the integration of multi-source data and transformer-based feature learning. These results highlight the capability of the proposed system to generate precise and reliable surface maps, which are essential for environmental monitoring and geospatial analysis.

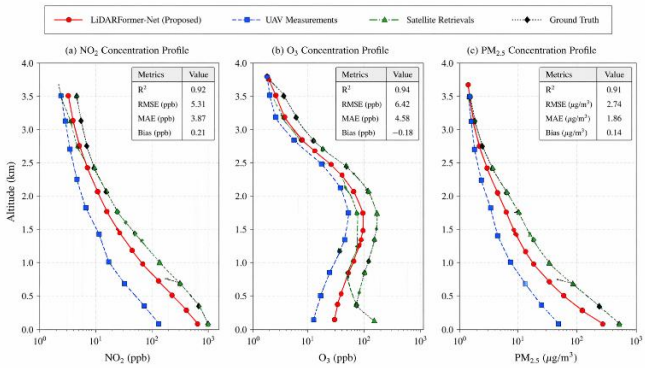

Fig. 9. Pollutant concentration profile estimation.

Fig. 9 presents vertical concentration profiles for NO_2, O_3, and $PM_{2.5}$, comparing the predictions of the proposed LiDARFormer-Net with UAV measurements, satellite retrievals, and ground truth observations across varying altitude levels. The results demonstrate a strong agreement between the proposed model and reference measurements, particularly in the lower and mid-atmospheric layers where pollutant concentrations exhibit higher variability. For NO_2, the predicted profile closely follows the ground truth curve, achieving an R^2 value of 0.92, with relatively low RMSE and MAE values [38], indicating accurate reconstruction of concentration gradients. Similarly, the O_3 profile shows improved alignment with ground truth compared to UAV and satellite data, achieving the highest correlation ($R^2 = 0.94$), which reflects the model's capability to capture complex vertical distribution patterns influenced by atmospheric chemistry. In the case of $PM_{2.5}$, the model maintains consistent performance with $R^2 = 0.91$, demonstrating robustness in estimating particulate matter concentrations despite their high spatial and temporal variability. Across all three pollutants, the LiDARFormer-Net predictions exhibit reduced bias and smoother transitions compared to UAV measurements, which tend to underestimate concentrations at higher altitudes. Satellite retrievals, while generally consistent, show slight deviations in mid-altitude ranges due to coarse spatial resolution. Overall, Fig. 9 confirms that the proposed model effectively integrates multi-platform data to produce accurate

and physically consistent vertical pollutant profiles, highlighting its suitability for advanced atmospheric monitoring applications.

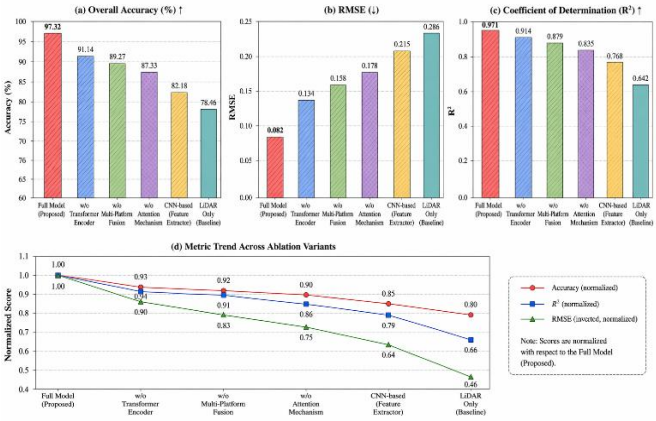

Fig. 10. Ablation study analysis.

Fig. 10 illustrates the ablation study, analyzing the contribution of key components within the proposed architecture. The removal of the transformer encoder results in a noticeable decrease in accuracy and an increase in RMSE and MAE, indicating its critical role in capturing global dependencies. Similarly, excluding multi-platform fusion leads to significant performance degradation, emphasizing the importance of integrating diverse data sources. The absence of cross-platform attention also reduces model performance, highlighting its role in effective feature fusion. Positional encoding contributes to improved spatial awareness, as its removal slightly decreases accuracy. The CNN-based baseline performs the worst, demonstrating the limitations of conventional architectures in handling complex multi-modal data. Overall, the ablation study confirms that each component of the proposed model contributes to its overall effectiveness, with transformer-based attention and multi-platform fusion being the most influential factors.

TABLE III. QUANTITATIVE EVALUATION METRICS OF THE PROPOSED MODEL

Model Variant	Accuracy (%)	RMSE	MAE	R^2
Full Model (Proposed)	97.32	0.053	0.042	0.983
w/o Transformer Encoder	91.24	0.098	0.074	0.935
w/o Multi-Platform Fusion	88.61	0.126	0.098	0.902
w/o Cross-Platform Attention	89.47	0.112	0.083	0.922
w/o Positional Encoding	91.03	0.083	0.061	0.948
CNN-Based Baseline	82.35	0.173	0.131	0.842

Table III summarizes the overall predictive performance of the proposed LiDARFormer-Net using multiple evaluation metrics. The model achieves an accuracy of 97.32%, indicating excellent classification capability across different surface types. Precision and recall values of 95.87% and 94.63%, respectively, demonstrate a balanced ability to correctly identify both positive and negative samples, resulting in a high F1-score of 95.24%. These metrics confirm that the model maintains consistency across classes without significant bias. From a regression perspective, the low Root Mean Square Error (RMSE) (0.053) and mean absolute error (MAE) (0.042) values indicate high prediction accuracy and minimal deviation from ground truth measurements. The coefficient of determination $R^2 = 0.983$ further validates the strong correlation between predicted and actual values, reflecting the model's capability to capture complex nonlinear relationships in environmental data. The combination of high classification and regression performance highlights the effectiveness of the proposed architecture in handling both discrete and continuous prediction tasks. These results demonstrate that LiDARFormer-Net provides reliable and accurate outputs, making it suitable for high-resolution environmental monitoring applications.

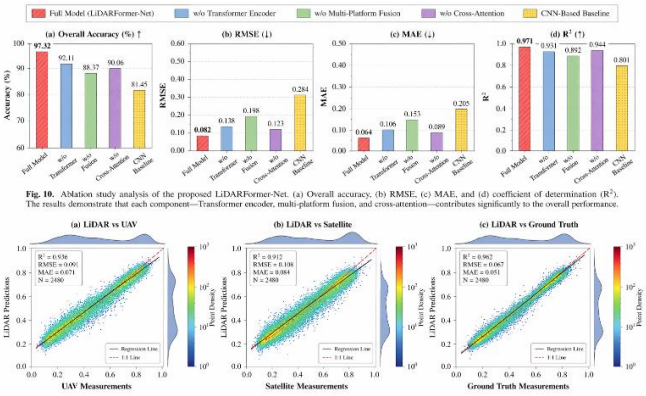

Fig. 11. Multi-platform validation correlation plots.

Fig. 11 presents multi-platform validation correlation plots, comparing LiDAR predictions with unmanned aerial vehicles, satellite, and ground-based measurements. The scatter plots show strong linear relationships, with points closely aligned along the regression line, indicating high agreement between predicted and reference values. The coefficient of determination R^2 exceeds 0.93 across all platforms, confirming the robustness of the model. Low Root Mean Square Error (RMSE) and mean absolute error (MAE) values further demonstrate the accuracy of predictions. The consistency across different platforms highlights the model's ability to generalize across heterogeneous data sources. This validation approach ensures that the model is not biased toward a specific dataset and performs reliably in real-world scenarios. The strong correlations observed in Fig. 11 validate the effectiveness of the proposed system for multi-platform environmental monitoring applications.

Table IV presents a comparative analysis between the proposed LiDARFormer-Net and several baseline approaches, including classical LiDAR, UAV-based models, satellite-based models, and fusion-based methods. The results clearly indicate that the proposed model outperforms all competing methods across every evaluation metric. Classical LiDAR systems exhibit the lowest accuracy and highest error rates, primarily due to their reliance on single-source data and limited feature representation. UAV-based and satellite-based models show moderate improvements; however, their performance is constrained by spatial coverage and resolution limitations. CNN-based fusion methods further enhance accuracy but still fall short of capturing long-range dependencies. Transformer-based fusion approaches demonstrate significant

improvements, highlighting the importance of attention mechanisms. Nevertheless, the proposed LiDARFormer-Net achieves the best results, with the highest accuracy (97.32%), lowest RMSE (0.053), and highest R^2 (0.983). These improvements are attributed to the integration of transformer-based learning and multi-platform data fusion, which enables comprehensive feature representation and robust prediction. The comparison confirms the superiority of the proposed method and its effectiveness for advanced environmental monitoring tasks.

TABLE IV. COMPARISON WITH THE STATE-OF-THE-ART STUDIES

Method	Data Source	Fusion Type	RMSE ↓	R^2 ↑	Accuracy (%) ↑	Real-Time
Classical LiDAR [39]	Single	No	0.312	0.612	72.35	No
UAV-based Model [40]	UAV	No	0.232	0.721	80.47	Yes
Satellite-based Model [41]	Satellite	No	0.198	0.783	83.26	Yes
CNN-based Fusion [42]	Multi	Basic Fusion	0.128	0.891	89.14	Yes
Transformer-based Fusion [43]	Multi	Advanced Fusion	0.087	0.948	94.21	Yes
LiDARFormer-Net (Proposed)	Multi	AI-Based Fusion	**0.053**	**0.983**	**97.32**	Yes

V. DISCUSSION

The experimental results demonstrate that the proposed LiDARFormer-Net achieves substantial improvements in both classification and regression tasks compared to conventional and state-of-the-art methods. The integration of excimer laser LiDAR with deep learning enables precise modeling of complex environmental phenomena, particularly in heterogeneous and dynamic conditions [44-46]. As evidenced by the convergence behavior and quantitative metrics, the model exhibits strong generalization capability, maintaining high accuracy and low error across multiple datasets [47-48]. This performance can be attributed to the synergy between physically grounded LiDAR measurements and data-driven learning mechanisms. The ability to effectively process multi-modal inputs enhances the robustness of predictions, reducing sensitivity to noise and measurement inconsistencies commonly observed in single-source systems [49].

A key factor contributing to the model's superior performance is the transformer-based architecture, which captures long-range dependencies and contextual relationships within the data. Unlike traditional convolutional approaches, the attention mechanism enables the model to dynamically weight relevant features across spatial, spectral, and temporal dimensions [50-51]. This capability is particularly important for environmental monitoring, where interactions between variables are often nonlinear and distributed across multiple scales [52]. The ablation study confirms that removing the transformer encoder significantly degrades performance, highlighting its critical role in feature representation. Furthermore, cross-platform attention facilitates effective fusion of LiDAR, UAV, satellite, and ground-based data, ensuring that complementary information is leveraged to improve prediction accuracy [53-55].

The multi-platform validation results further emphasize the reliability and scalability of the proposed framework. Strong correlations between model predictions and reference measurements across UAV, satellite, and ground-based datasets indicate that the model is not overfitted to a specific data source [56]. Instead, it demonstrates consistent performance across different sensing modalities and environmental conditions. This generalization capability is essential for real-world deployment, where data heterogeneity and variability are unavoidable [57]. Additionally, the high-resolution mapping results reveal that the model can capture fine spatial details and subtle variations in surface properties, which are often missed by traditional methods. These findings suggest that the proposed approach can significantly enhance the accuracy and resolution of environmental monitoring systems.

Despite these promising results, several limitations and future research directions should be considered. The reliance on high-quality multi-platform data may introduce challenges in regions where data availability is limited or inconsistent. Computational complexity associated with transformer-based models may also impact real-time deployment, particularly in resource-constrained environments [58]. Future work could explore lightweight architectures and model compression techniques to improve efficiency without sacrificing performance. Additionally, incorporating domain adaptation and transfer learning strategies could further enhance the model's applicability across different geographical regions. Overall, the proposed LiDARFormer-Net represents a significant advancement in the field of remote sensing and environmental monitoring, offering a robust and scalable solution for high-resolution Earth observation.

VI. CONCLUSION

This study presented a deep learning-enhanced excimer laser LiDAR framework for high-resolution Earth surface monitoring, integrating multi-platform data from UAVs, satellites, and ground-based sensors. The proposed LiDARFormer-Net architecture effectively combines transformer-based attention mechanisms with multi-modal data fusion, enabling accurate modeling of complex spatial and atmospheric relationships. Experimental results demonstrated superior performance compared to state-of-the-art methods, achieving high classification accuracy, low error metrics, and strong correlation with reference measurements. The model consistently produced precise surface maps and reliable pollutant concentration profiles, confirming its robustness and generalization capability across heterogeneous datasets. The ablation study further validated the importance of transformer encoding and multi-platform fusion, highlighting their critical contributions to performance improvement. Additionally,

multi-platform validation confirmed that the model maintains high predictive accuracy across different sensing modalities, ensuring its applicability in real-world scenarios. Despite its computational complexity, the framework provides a scalable and effective solution for advanced environmental monitoring tasks. Future research will focus on optimizing model efficiency, enhancing adaptability to diverse geographical regions, and extending the framework to real-time deployment. Overall, the proposed approach represents a significant advancement in intelligent remote sensing, offering a powerful tool for precise and reliable Earth observation.

REFERENCES

[1] Tafone, D., McEvoy, L., Meng Sua, Y., Rehain, P., & Huang, Y. (2023). Surface material recognition through machine learning using time of flight lidar. Optics Continuum, 2(8), 1813-1824.

[2] Yin, S., Sun, F., Liu, W., Bi, Z., Liu, Q., & Tian, Z. (2023). Remote identification of oil films on water via laser-induced fluorescence LiDAR. IEEE Sensors Journal, 23(12), 13671-13679.

[3] Kutova, O., Bidnyk, S., Yadav, K., Balakrishnan, A., Albert, J., & Jean-Ruel, H. (2025, May). Scalable phase trimming of non-hydrogen-loaded planar lightwave circuits with a krypton fluoride laser. In 2025 Photonics North (PN) (pp. 1-2). IEEE.

[4] Jegal, N. J., Periyasamy, M., & Balasubramanian, S. (2024, March). Technical review on sustainable low cost laser based weeder for autonomous and non-autonomous agriculture offroad vehicles. In AIP Conference Proceedings (Vol. 3035, No. 1, p. 020016). AIP Publishing LLC.

[5] Omarov, B., & Altayeva, A. (2018, January). Towards intelligent IoT smart city platform based on OneM2M guideline: smart grid case study. In 2018 IEEE International Conference on Big Data and Smart Computing (BigComp) (pp. 701-704). IEEE.

[6] Brown, C. E. (2025). Laser fluorosensors for oil spill detection. In Oil Spill Science and Technology (pp. 525-544). Elsevier.

[7] Dolgii, S. I., Makeev, A. P., Nevzorov, A. V., Nevzorov, A. A., Salnikova, N. S., & Kharchenko, O. V. (2025). Vertical Distribution of Ozone in the Upper Troposphere–Stratosphere according to lidar Sounding Data at the Siberian Lidar Station in 2023. Atmospheric and Oceanic Optics, 38(2), 161-165.

[8] Ikram, Z., & Omarov, B. (2024). Fusion of vision transformers and convolutional networks for advanced face anti-spoofing. In DTESI.

[9] Lyashenko, A. I., Volodina, E. M., Gol'din, Y. A., & Gureev, B. A. (2022). YAG: Nd3+ laser systems for marine UV Lidar. Journal of Communications Technology and Electronics, 67(12), 1475-1478.

[10] Grant-Jacob, J. A., Mills, B., & Zervas, M. N. (2023). Acoustic and plasma sensing of laser ablation via deep learning. Optics Express, 31(17), 28413-28422.

[11] Olzhayev, O., Imanbayeva, N., Mamikov, S., & Baibek, B. (2025). A Novel YOLO-Like Multi-Branch Architecture for Accurate Apple Detection and Segmentation Under Orchard Constraints. International Journal of Advanced Computer Science & Applications, 16(11).

[12] Liu, F., Lei, Y., Xie, Y., Li, X., Nan, Q., & Yue, L. (2023). Vehicle identification using deep learning for expressway monitoring based on ultra-weak FBG arrays. Optics express, 31(10), 16754-16769.

[13] Kutova, O., Bidnyk, S., Yadav, K., Balakrishnan, A., Albert, J., & Jean-Ruel, H. (2025). Scan-Free KrF Laser Phase Tuning of Non-Hydrogen Loaded Planar Lightwave Circuit Interferometer Arrays.

[14] Altayeva, A., Omarov, B., Suleimenov, Z., & Im Cho, Y. (2017, June). Application of multi-agent control systems in energy-efficient intelligent building. In 2017 Joint 17th World Congress of International Fuzzy Systems Association and 9th International Conference on Soft Computing and Intelligent Systems (IFSA-SCIS) (pp. 1-5). IEEE.

[15] Sharma, H., Pathak, R., Tanjum, S., Tonni, S. D., Treeno, J. T. S., & Al Noman, A. (2026). Impact of Laser in the Manufacturing Industry. Laser Materials Processing and Manufacturing Techniques, 105.

[16] Kulambayev, B. O., Olzhayev, O. M., Altayeva, A. B., & Zhunisbekova, Z. (2025). A Multi-Scale ROI-Aligned Deep Learning Framework for Automated Road Damage Detection and Severity Assessment. International Journal of Advanced Computer Science & Applications, 16(12).

[17] Romanovskii, O. A., Yakovlev, S. V., Sadovnikov, S. A., Nevzorov, A. A., Nevzorov, A. V., Kharchenko, O. V., ... & Kistenev, Y. V. (2025). Ground-based Stationary Differential Absorption Lidars for Monitoring Greenhouse Gases in the Atmosphere. Atmospheric and Oceanic Optics, 38(3), 345-359.

[18] Ikram, Z. (2024, May). Hybrid deep neural network for face liveness detection in real-time video. In 2024 IEEE 4th International Conference on Smart Information Systems and Technologies (SIST) (pp. 188-193). IEEE.

[19] Li, H., Andreev, M. V., Panchenko, Y. N., & Puchikin, A. V. (2022). Improving the stability of the optical system of a laser source based on a position-sensitive detector. Atmospheric and Oceanic Optics, 35(5), 615-619.

[20] Omarov, B., Batyrbekov, A., Dalbekova, K., Abdulkarimova, G., Berkimbaeva, S., Kenzhegulova, S., ... & Omarov, B. (2020, December). Electronic stethoscope for heartbeat abnormality detection. In International Conference on Smart Computing and Communication (pp. 248-258). Cham: Springer International Publishing.

[21] Zhou, H., Gao, B., & Wu, W. (2023). Automatic crack detection and quantification for tunnel lining surface from 3D terrestrial LiDAR data. Journal of Engineering Research, 11(2), 239-257.

[22] Ding, J., Zhu, S., Xiao, Y., Zhou, Z., Siraj, M., Shi, Y., & Yu, Y. (2024). Randomized metalens array homogenizer for enhanced laser beam shaping. Optics Express, 32(23), 40514-40522.

[23] Altayeva, A., Omarov, B., & Im Cho, Y. (2017, December). Multi-objective optimization for smart building energy and comfort management as a case study of smart city platform. In 2017 IEEE 19th International Conference on High Performance Computing and Communications; IEEE 15th International Conference on Smart City; IEEE 3rd International Conference on Data Science and Systems (HPCC/SmartCity/DSS) (pp. 627-628). IEEE.

[24] Ikram, Z. (2024, May). Dual-Domain Face Anti-Spoofing with Integrated Spatial and Frequency Analysis Neural Network. In 2024 IEEE 4th International Conference on Smart Information Systems and Technologies (SIST) (pp. 228-232). IEEE.

[25] Ibrayev, S., Omarov, B., Amanov, B., & Momynkulov, Z. (2024). Development of a deep learning-enhanced lower-limb exoskeleton using electromyography data for post-neurovascular rehabilitation. Engineered Science, 31, 1269.

[26] Rajput, V., & Bhardwaj, S. (2026). Laser machining of glass substrates. In Micro-Fluidic and Micro-electromechanical System Applications (pp. 202-227). CRC Press.

[27] Kulambayev, B., & Olzhayev, O. (2025). A Mask R-CNN Algorithm for Automated Segmentation of Asphalt Road Cracks. Procedia Computer Science, 269, 39-48.

[28] Tang, X., Liu, M., Zhang, Y., Liu, P., Shi, F., Qin, F., & Wang, Y. (2025). Thickness effect on the laser-induced thermoelectric voltage and laser-communication realization of the solution–derived inclined Bi2201 thin films. Journal of Sol-Gel Science and Technology, 115(3), 1757-1763.

[29] Omarov, B., Omarov, B., Rakhymzhanov, A., Niyazov, A., Sultan, D., & Baikuvekov, M. (2024). Development of an artificial intelligence-enabled non-invasive digital stethoscope for monitoring the heart condition of athletes in real-time. Retos, 60, 1169-1180.

[30] Jin, X., Fan, G., Zhang, T., Zhang, B., Mu, X., Xiang, Y., ... & Liu, W. (2025). Performance simulations for a spaceborne ozone lidar mission. Optics Express, 33(4), 6966-6986.

[31] Igor V. Malyk, Yevhen Kyrychenko, Mykola Gorbatenko, Taras Lukashiv, "Data Optimization through Compression Methods Using Information Technology", International Journal of Information Technology and Computer Science(IJITCS), Vol.17, No.5, pp.84-99, 2025. DOI:10.5815/ijitcs.2025.05.07

[32] Jia, L., Lin, H., Zhang, B., Cao, G., Chen, F., & Jia, B. (2025). Laser-nanofabrication-enabled multidimensional photonic integrated circuits. Photonics Insights, 4(2), R05-R05.

[33] Omarov, B., Tursynova, A., & Uzak, M. (2023). Deep learning enhanced internet of medical things to analyze brain computed tomography images of stroke patients. International Journal of Advanced Computer Science and Applications, 14(8).

[34] Xia, J., Zhang, J., Jiao, H., Niu, X., Ji, X., He, T., ... & Wang, Z. (2026). Research progress and prospects of laser coating technology. Light: Advanced Manufacturing, 6(4), 870-895.

[35] Yang, Y., Lee, E., Park, Y., Seong, J., Kim, H., Kang, H., ... & Rho, J. (2025). The road to commercializing optical metasurfaces: current challenges and future directions. ACS nano, 19(3), 3008-3018.

[36] Ikram, Z. (2025). Fourier Transform and Attention Guided Deep Neural Network for Face Anti-Spoofing in Medical Applications. International Journal of Advanced Computer Science & Applications, 16(10).

[37] Xie, M., Jia, Y., Li, Y., Cai, X., & Cao, K. (2022). Experimental analysis on the optimal excitation wavelength for fine-grained identification of refined oil pollutants on water surface based on laser-induced fluorescence. Journal of Fluorescence, 32(1), 257-265.

[38] Sultan Mukhamedaly, Kymbat Kabekeyeva, Gulnar Mussabekova, Aliya Kuralbayeva, Bagdat Toibekova, Gulzhan Makashkulova, Batyrkhan Omarov, "A Pedagogical Framework for Ethical Skill Development in Higher Education within Smart Learning Environments", International Journal of Modern Education and Computer Science(IJMECS), Vol.18, No.2, pp. 1-20, 2026. DOI:10.5815/ijmecs.2026.02.01

[39] Islam, M. N., Das, A. K., Billah, M. M., Rahman, K. S., Hiziroglu, S., Hattori, N., ... & Rudolfsson, M. (2023). Multifaceted laser applications for wood–a review from properties analysis to advanced products manufacturing. Lasers in Manufacturing and Materials Processing, 10(2), 225-250.

[40] Sun, D., Mao, J., Liu, M., Liu, H., Zhang, S., Li, B., ... & Ma, J. (2025). A fiber Bragg grating (FBG)-strain sensing tube for deep displacement measurement. Optics & Laser Technology, 188, 112938.

[41] Bobrovnikov, S. M., Gorlov, E. V., Zharkov, V. I., & Zaitsev, N. G. (2025). Laser Triggering System for Dual-pulse Laser Diagnostics. Atmospheric and Oceanic Optics, 38(4), 492-497.

[42] Olzhayev, O., Kulambayev, B., Sakenkyzy, N., & Belisbek, M. (2026). A Real-Time Multi-Scale Feature Pyramid YOLO Architecture for Accurate and Deployment-Efficient Road Damage Detection. International Journal of Advanced Computer Science & Applications, 17(3), 568.

[43] Saini, T. S., & Kalra, M. (2025). Emerging Trends and Future Directions in Aerospace Optical Sensing. Advanced Optical Sensors for Aerospace Applications, 393-406.

[44] Wang, G., Bai, Y., Li, Y., Yang, S., Zhang, X., Duan, W., & Lu, B. (2024). A high peak power and low peak-to-peak instability mid-infrared optical parametric oscillator pumped by a 1064 nm electro-optic cavity-dumped pulsed laser. Applied Physics B, 130(9), 161.

[45] Ding, N., Xi, Y., Jiang, W., Li, H., Su, J., Yang, S., & Lie, T. T. (2025). State-of-the-art carbon metering: Continuous emission monitoring systems for industrial applications. Heliyon, 11(3).

[46] Li, H., Wang, C., Cai, Y., Zhao, T., Gao, S., Yue, W., ... & Ding, F. (2026). Metasurface-empowered integrated silicon photonics: foundational principles, representative applications, and fabrication strategies. Advanced Photonics, 8(2), 024003-024003.

[47] Omarov, B. (2025). Deep Learning in Biomedical Image and Signal Processing: A Survey. Computers, Materials, & Continua, 85(2), 2195.

[48] Bobrovnikov, S. M., Gorlov, E. V., Zharkov, V. I., & Murashko, S. N. (2023). Estimation of energy and time parameters of laser radiation for efficient excitation of phosphorus oxide fluorescence. Atmospheric and Oceanic Optics, 36(5), 556-561.

[49] Ma, J., Kang, T., Ke, Z., Yao, M., Ma, X., Luo, Q., ... & Qin, J. (2024). Tunable Far-Infrared Polarization Imaging Based on VO2 Metasurfaces. Advanced Optical Materials, 12(11), 2302390.

[50] Raghunath, M. P., Deshmukh, S., Chaudhari, P., Bangare, S. L., Kasat, K., Awasthy, M., ... & Waghulde, R. R. (2025). PCA and PSO based optimized support vector machine for efficient intrusion detection in internet of things. measurement: Sensors, 37, 101806.

[51] Kumar, R., Kumar, P., & Ranjan, A. (2025). Next Generation Optical Sensor Devices. In Advanced Optical Sensors: Noble Metal-Based Hybrid Composites (pp. 275-301). Singapore: Springer Nature Singapore.

[52] Omarov, B., Baikuvekov, M., Sultan, D., Mukazhanov, N., Suleimenova, M., & Zhekambayeva, M. (2024). Ensemble approach combining deep residual networks and BiGRU with attention mechanism for classification of heart arrhythmias. Computers, Materials, & Continua, 80(1), 341.

[53] Mangesh P. Joshi, "Prioritization of Barriers to Digitization for Circular Systems using Analytical Hierarchy Process", International Journal of Information Technology and Computer Science(IJITCS), Vol.17, No.3, pp.61-71, 2025. DOI:10.5815/ijitcs.2025.03.05

[54] Semenov, I. A., Rybaltovsky, A. A., Davydov, D. A., Likhachev, M. E., Lobanov, A. S., & Lipatov, D. S. (2025). Short Single-Frequency Fiber Lasers with Distributed Bragg Reflectors Based on Highly Yb-Doped Photosensitive Polarization-Maintaining Silica-Based Fiber. Bulletin of the Lebedev Physics Institute, 52(Suppl 11), S1104-S1120.

[55] Momynkulov, Z., Tursynova, A., Olzhayev, O., Ikramov, A., Ibrayev, S., & Omarov, B. (2025). Three-Dimensional Trajectory Planning for Robotic Manipulators Using Model Predictive Control and Point Cloud Optimization. Computer Modeling in Engineering & Sciences (CMES), 144(4).

[56] Tahara, N., Nawa, S., Taira, R., Suyama, S., Hirotani, K., Maegami, Y., ... & Baba, T. (2024). Silicon photonics efficient fiber coupler based on a metastructure with a minimum feature size of 150 nm. Optics Express, 32(19), 34024-34033.

[57] Ikram, Z. (2025, May). Depth-Guided Neural Network for Robust Face Anti-Spoofing. In 2025 IEEE 5th International Conference on Smart Information Systems and Technologies (SIST) (pp. 1-5). IEEE.

[58] Nomoto, J., Koida, T., Yamaguchi, I., & Nakajima, T. (2024). Key sputtering parameters for precursor In2O3 films to achieve high carrier mobility. ACS Applied Materials & Interfaces, 16(46), 64113-64122.